Synthesis and solvent driven self-aggregation studies of *meso*-"*C*-glycoside"-porphyrin derivatives†

Petr Štěpánek,[a] Mykhaylo Dukh,[a] David Šaman,[a] Jitka Moravcová,[b] Ladislav Kniežo,[b] Donato Monti,[c] Mariano Venanzi,[c] Giovanna Mancini[d] and Pavel Drašar*[a,b]

Received 6th November 2006, Accepted 8th January 2007
First published as an Advance Article on the web 31st January 2007
DOI: 10.1039/b616096d

New types of porphyrin derivatives bearing "*C*-glycoside" moieties, either in 5,10,15,20- or in 5,15-*meso*-positions, were prepared and fully characterized. The presence of the glycosidic groups imparts to the title macrocycles, besides an amphiphilic character, a clear tendency to form chiral suprastructures upon solvent-driven self-aggregation in different aqueous–organic solvent mixtures. Supra-assembly phenomena, in terms of the size and morphology of the resulting structures, as well as their kinetics of aggregation, were studied by UV-visible, fluorescence, resonance light scattering (RLS), and CD spectroscopy, indicating that the morphology of the aggregates depends strongly on the structure of the porphyrin rings, and on the bulk conditions of aggregation.

Introduction

The control of the symmetry and chirality of important receptors is a key issue in modelling natural pathway-mimics in the chemical laboratory today and in nanodevice design tomorrow. Supramolecular chemistry, as defined by Jean-Marie Lehn,[1] is the "the chemistry beyond the molecules, bearing on the organized entities of higher complexity that result on the association of two or more chemical species held together by intermolecular forces."

Generally, compounds in which the active bearer of property (functiophore, pharmacophore, chromophore, and so on) is conjugated with a vector such as a peptide,[2–4] nucleotide,[5] borane,[6] saccharide[7–17] or combined[18] moieties, are of great interest. The introduction of a chiral hydroxylated vector, such as, for example, a carbohydrate group, into a porphyrin frame, would impart to such derivatives promising molecular recognition features, *i.e.* hydrogen bonds, with appealing stereoselective properties brought by the presence of carbon stereogenic centres.[17,19] Porphyrin–carbohydrate conjugates, although based on different synthetic philosophies, have been found to have important applications as sensitizers in photodynamic therapy (PDT) for cancer treatment, and for other therapeutic utilisation.[20] Moreover, these derivatives have been recognized to present other important features, such as incorporation into cell membrane models,[21] interaction with DNA and nucleotides[22] or electrochemical[23] properties, which makes them suitable for utilization in catalysis[24–27] or in analytical chemistry.[28,29]

The aim of our project is to implement into our supramolecular synthon (a porphyrin building block) a chiral recognition and/or discrimination feature/function. Hence, we adopted a very simple philosophy entailing the functionalisation of the known porphyrin platform by tailored, well-functioning chiral ligands with easily tunable properties such as, for example, steroids, peptides or carbohydrates.[30,31] A straightforward procedure would then concern the construction of a porphyrin–saccharide conjugate, where the "sugar" moiety is linked to the macrocycle in a *meso*-position[32–34] with direct and robust covalent C–C bonds, which, differing from the previously reported *O*-glycosidic bond, is stable towards hydrolytic or enzymatic degradation. Furthermore, the "sugar" moiety should impart to the resulting porphyrin platform tunable polar/lipophilic properties, depending on the level of protection and/or hydroxylation, and on the OH groups spatial orientation (stereo- and regiochemistry). This issue would be also of great importance for the development of biological-like receptors, able to work in aqueous media.[19,35] Another important point is that the presence of chiral appended functionalities (*i.e.* sugar moieties) would impart to these substrates interesting stereoselective properties, in terms of, for example, chiral recognition, self-recognition and aggregation (*cf.* ref. 19, for example).

Results and discussion

The synthetic part of this work exploited several attempts to synthesize the *meso*-"*C*-glycosylated" porphyrins ("*C*-glycoside" is a trivial name for a compound in which an oxygen atom of the glycosidic bond is replaced by a methylene group. Similar compounds in which the sugar moiety is directly connected with more than one methylene unit are sometimes trivially called pseudo-*C*-glycosides[36]). There are several papers reporting on the synthesis of porphyrins with the "carbohydrate" moiety bonded directly,[32,34] either by a heteroatom[37–39] or by a spacer.[39] To the best of our knowledge, we present in this paper the first example of a compound in which a "sugar moiety" is linked to the methylene bridge of a porphyrin ring.

[a]*Institute of Organic Chemistry and Biochemistry, AS CR, Flemingovo nám. 2, CZ-166 10, Praha 6, Czech Republic. E-mail: Pavel.Drasar@vscht.cz*
[b]*Institute of Chemical Technology, Technická 5, CZ-166 28, Praha 6, Czech Republic*
[c]*Dipartimento di Scienze e Tecnologie Chimiche, Univ. Roma "Tor Vergata", I-00133, Rome, Italy*
[d]*IMR-CNR, c/o Dip. Chim., Univ. Roma "La Sapienza", I-00185, Rome, Italy*

† Electronic supplementary information (ESI) available: NMR data and experimental details. See DOI: 10.1039/b616096d

Two basic strategies were used: one, leading to a porphyrin type with all four *meso*-positions substituted with identical ligand (type **A**), relies on direct cyclization of "sugar" aldehydes with pyrrole, whereas the second, based on sequential construction from the dipyrrylmethane precursors, yields to porphyrin derivatives with 5,15-*meso*-substitution pattern (type **B**).

As far as the former strategy is concerned, aldehydes **1** (ref. 40) and **3** (ref. 41) were used as building blocks in direct condensation with pyrrole in dichloromethane (Lindsey conditions[42]), to give **A**-type *meso*-substituted porphyrins in very good 18 and 36% yields (for **2** and **4**, respectively, Scheme 1).

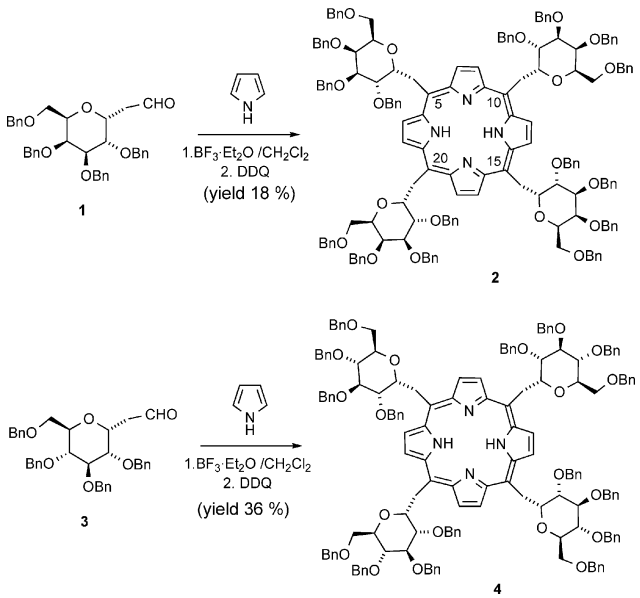

Scheme 1 Reaction of aldehydes with pyrrole under catalysis with $BF_3{\cdot}Et_2O$.

The modular synthesis of **B**-type porphyrins was accomplished by following a well-established 2 + 2 MacDonald type procedure: dipyrryl derivatives **5** and **6** can be obtained by condensation of aldehydes **1** and **3** with pyrrole in dichloromethane in the presence of trifluoroacetic acid (TFA) in good yields, *i.e.*, 49 and 84% for "D-*galacto*" and "D-*gluco*" derivatives **5** and **6**, respectively (Scheme 2). The products obtained are relatively stable and can be purified by flash chromatography.

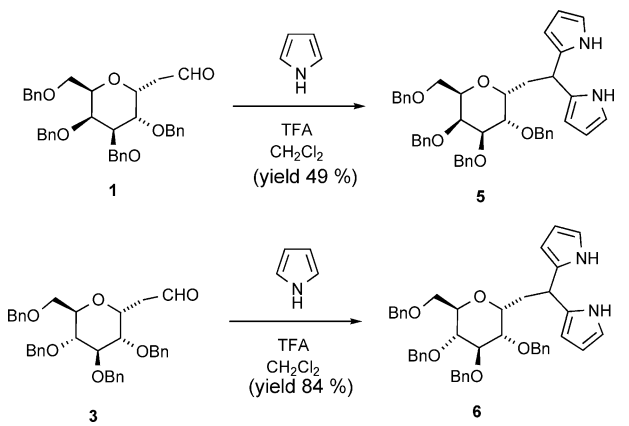

Scheme 2 Reaction of aldehydes with pyrrole under catalysis with TFA.

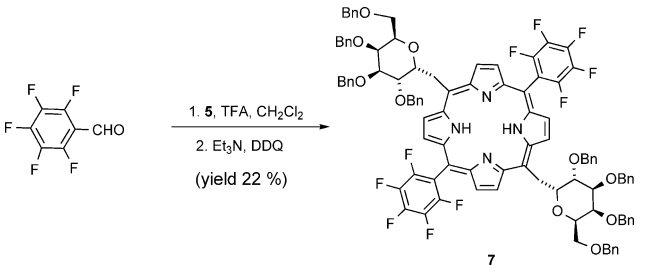

Scheme 3 Condensation of dipyrrylmethane **5** with pentafluorbenzaldehyde.

Hence the **B**-type porphyrin derivative **7** was prepared by acid catalyzed (TFA) condensation of dipyrryl derivative **5** with pentafluorbenzaldehyde in dichloromethane and subsequent *in situ* DDQ oxidation, to yield porphyrin **7** in a good 22% yield (Scheme 3). The pentafluorophenyl substitution was selected for two reasons. Firstly, the moiety is very lipophilic and, thus, rather different from a "carbohydrate" one (not considering different binding possibilities). The second reason was the reactivity of the fluorine in position of the C-4 of benzene ring, which is utilized for substitution reactions and binding to the solid phase.

Similar reactions carried out on dipyrryl derivative **6** gave a mixture of porphyrin derivatives with very similar structures, in low yields. Spectral investigation (MS and NMR), gave good evidence of the presence of porphyrin **8** as one of the main components (Scheme 4), together with other porphyrinic material with a larger MS (MALDI) ion peak at m/e 2085.72 (which had typical a UV-vis absorption, too). Here, we were unable to get a sufficient amount of the pure compounds and the reaction will be the subject of further investigations—the details will be reported elsewhere. It could be suggested that the compound is a porphyrin with one pentafluorophenyl and three "*C*-glycosides", obtained by the scrambling phenomena described by Lindsey;[43] such a compound should have the chemical formula: $C_{131}H_{123}F_5N_4O_{15}$, with the exact mass: 2086.89.

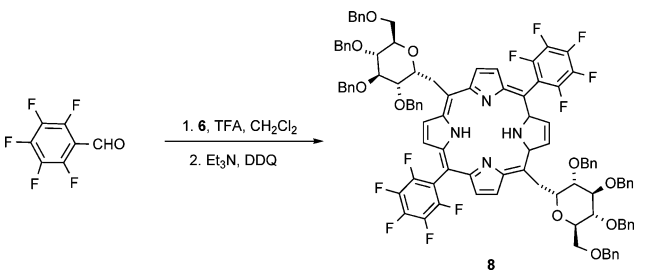

Scheme 4 Condensation of dipyrryl derivative **6** to porphyrin **8**.

The best protocol to obtain porphyrin **7** selectively entails the condensation of pentafluorphenyldipyrrylmethane **9** (ref. 44) with sugar aldehydes **1** and **3**, followed by treatment with DDQ. The resulting reaction mixtures gave, in the case of starting aldehyde **1**, porphyrin **7** in a very good 27% yield (Scheme 5). In the case of aldehyde **3**, however, the reaction showed an outcome similar to that observed in the case of the reaction of the pentafluorbenzaldehyde and dipyrryl derivative **6** discussed above.

Debenzylation of this kind of complex structure could be a real problem.[18] However, we found that the only case of a successful attempt was that entailing the simple hydrogenation of **7** over

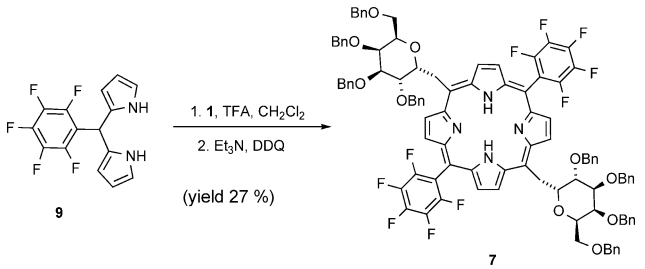

Scheme 5 Condensation of pentafluorphenyldipyrrylmethane **9** to porphyrin **7**.

palladium on charcoal, to give the fully hydroxylated derivative **10** in a 63% yield (Scheme 6). Characteristic UV-visible spectral patterns are reported in Fig. 1. These unprotected (free-OH) derivatives can be of importance for the preparation and the study of sugar-based, water-soluble tetrapyrrolic macrocycles.

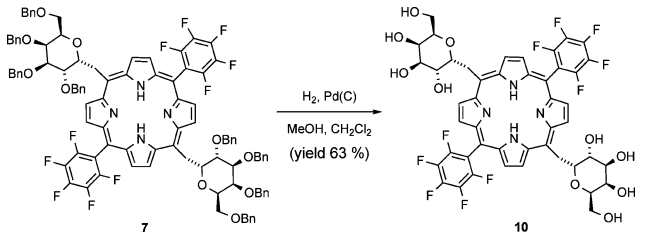

Scheme 6 Deprotection of porphyrin **7**.

The above-reported series of novel compounds were further studied on the basis of their properties and potential use as building blocks for more elaborate and functional architectures. This latter issue can be of striking importance for the development of supramolecular mimics of the enzyme machinery[45] of photosynthetic bacteria, or for sensor applications. We recently reported, in fact, that layered films of amphiphilic porphyrin derivatives are of importance in the construction of selective solid-state sensors for Hg^{2+} ions.[46]

The results show major differences in the chemical as well as physico-chemical properties of the compounds prepared, even at the same level of OH group protection, depending on the specific structure of the glycosidic peripheral functionalisation. Namely, several properties of compounds derived from "D-*gluco*" precursors do differ from those from "D-*galacto*" ones, which can be illustrated by their purification and reaction ability, *i.e.*, the differences observed can be ascribed to the occurrence of specific intermolecular interactions in solution. Chloroform solutions of the "sugar" substituted pyrroles and porphyrins in fact gave unexpected polarimetric measurements with rather high readings even in quite dilute solutions, which became stable only after a prolonged time (minutes to hours) from preparation, with no other apparent chemical change detected. This finding can be undoubtedly interpreted on the basis of the occurrence of self-aggregation phenomena between porphyrin macrocycles and at a lower level also in dipyrrole derivatives. We recently reported that the self-aggregation of chirally-functionalized porphyrin derivatives results in the formation of architectures characterized by well-defined supramolecular chirality.[47] A similar behavior can be surmised to be operative in this present case. In order to shed more light on this important issue, a series of detailed spectroscopic studies was carried out. For this initial study we selected two candidates, *i.e.*, porphyrins **2** and **7**, which were found to be the most promising in early investigations.[48] Other molecules are currently under study.

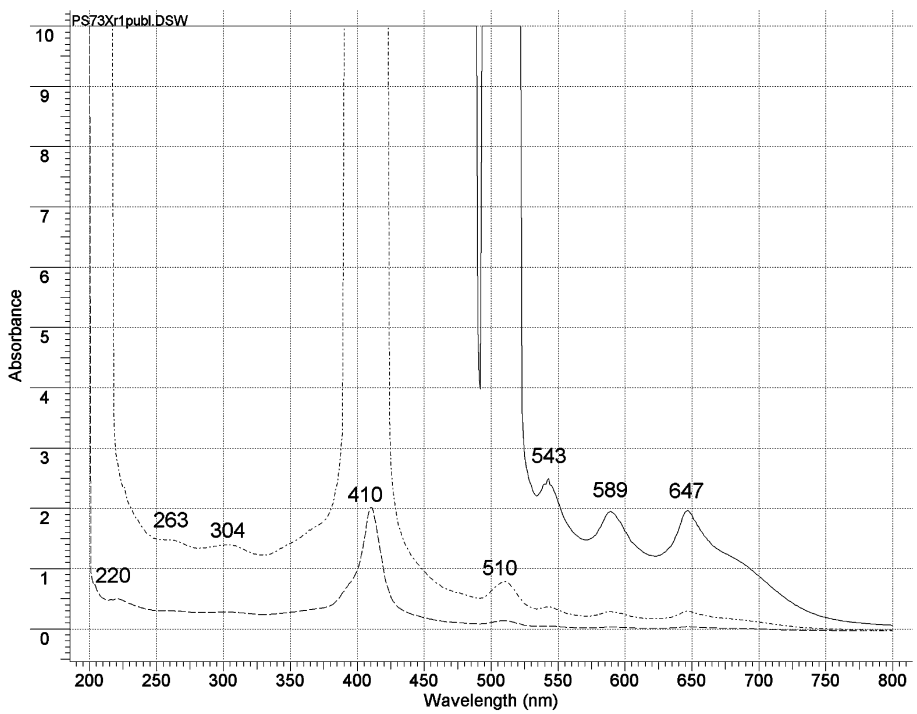

Fig. 1 Typical UV-vis spectral pattern of porphyrin **10** in methanol, showing a Sorret band at 410 nm and Q-bands from both sides (dash-and-dot line to dashed ×5, to solid ×40).

The title porphyrins **2** and **7**, differing in their peripheral substitution pattern (the former being substituted by four "glycosidic" groups, and the latter featuring two pentafluorophenyl rings and two "glycosidic" moieties in mutually alternating positions) would feature different properties, in terms of electronic and steric effects, and consequently, different self-aggregation properties. These tetrapyrrolic macrocycles show good solubility in either chlorinated and polar aprotic solvents such as DMSO, DMF and MeCN. The relative UV-visible spectra, at μM concentration, show a narrow Soret band (λ_{max} 422 and 416 nm, in chloroform, for **2** and **7**, respectively) indicating the solubilisation of the chromophores in the monomeric form. The hypsochromic shift of porphyrin derivative **7** is safely ascribable to the electron withdrawal effect of C_6F_5 moieties.[49] The aggregation behavior of the tetrapyrrolic macrocycles was studied in aqueous solvent mixtures, namely DMSO–water, DMF–water and MeCN–water, at different water proportions in μM concentrations. In all of the mixtures investigated, a hypochromic effect of the electronic bands was observed, ongoing through 0 to 100% water composition. A concomitant red shift of the absorption maxima is also evidenced. This indicates the occurrence of solvent-driven porphyrin aggregation, toward the formation of J-type, edge-to-edge, supramolecular architectures.[50] Evidently, the increasing of solvent polarity steers the onset of hydrophobic (*e.g.*, π–π) interaction among the aromatic porphyrin platforms. These results are graphically reported in Fig. 2, for the aggregation studies of **7** carried out in MeCN–H_2O. The nature of solutions (true/non-true; or solution/emulsion) was not examined.

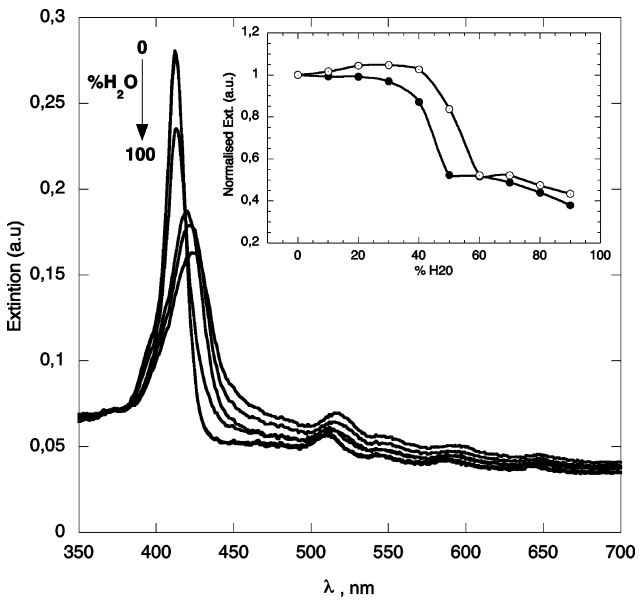

Fig. 2 UV-vis spectroscopic variation of **7**; 1.3 μM, in MeCN–H_2O solvent mixtures (uppermost curve: 0–40% H_2O; lowermost curve: 100% H_2O). Inset: "aggregation curves" for **2** (lower curve), and **7** (upper curve) 3.7 μM, at $T = 298$ K.

The intensity of the Soret bands is monitored upon changing the composition of solvent (v/v). (The term "extinction" is more appropriate than "absorbance" because of the presence of RLS contribution to UV visible and CD bands. For a discussion on this topic see ref. 51.) The solvent composition at which a sudden intensity drop occurs can be noted as the "critical aggregation solvent composition" (casc).[52] In this case, the term "casc" indicates a solvent composition at which the aggregation process becomes evident. At water compositions below this value, the aggregation is too slow to be appreciated (or even does not occur), whereas at higher values the aggregation is complete within the time of mixing. At this particular solvent composition, a detailed kinetic study can be conveniently carried out by means of conventional techniques (see the Experimental section). Similar results, in terms of spectral changes and "casc", are observed at higher porphyrin concentration, *i.e.*, 3.6 μM. Similar trends are observed in different aqueous solvent mixtures, namely DMSO–water and DMF–water. However, in these latter solvents, aggregation promoted at $H_2O >$ 60% v/v occurs with some cloudiness of the solution, indicating the formation of large, mesoscopic-sized porphyrin aggregates. The aggregation experiments, as far as this explorative stage is concerned, have then been focused on the case of MeCN–H_2O solvent mixtures, in which accurate conventional spectroscopic studies can be safely carried out. Detailed studies on the effect of different solvents are under investigation, and the results will be reported elsewhere.

Aggregation of porphyrin derivative **2** shows the "casc" at *ca.* 50% water content (Fig. 2, inset). The bis-pentafluorophenyl derivative **7** shows some differences in aggregation behaviour. Complete aggregation of the bis-pentafluorophenyl derivative **7** in fact occurs significantly at *ca.* 60% of water. This would be interpreted on the basis of the presence of C_6F_5-groups, which would be better solvated by H-bonding. Moreover, this latter macrocycle features a less-extended aromatic electronic surface, with respect to that of derivative **2**, resulting in the one set of π–π stacking interactions only at higher water proportions.

Fluorescence experiments confirm the formation of porphyrin aggregates in water-rich solvent mixtures. It is well known that porphyrin chromophores feature strong intensity emission in the 600–700 nm range, with a decay time, τ, of about 12 ns. In a typical experiment ($\lambda_{ex} = 518$ nm; $\lambda_{em} = 645$ nm), the emission of the porphyrin concerned (*i.e.*, **7** or **2**) is monitored in aqueous MeCN, at [P] = 1.1 μM. The fluorescence is strongly quenched upon increasing water proportion, indicating the formation of strongly electronically-coupled, non radiative porphyrin aggregates[53] (Fig. 3, inset). Remarkably, the drop in signal emission occurs at the same solvent composition found by UV-visible techniques, safely confirming the occurrence of the aggregation phenomena.

The formation of large porphyrin aggregates is further corroborated by resonance light scattering spectroscopy studies. This relatively new technique,[54] which is based on the enhancement of the scattering of light on the red edge of the Soret band, is strongly dependent on the size of porphyrin aggregates, the extent of electronic coupling between adjacent chromophores and their molar extinction coefficients. Indeed, light scattering experiments on aqueous MeCN solutions of either **2** and **7** show a gradual growth of the RLS signal on the Soret band region of the aggregates (*ca.* 430 nm; see Fig. 3) on increasing water proportion, with the intensity approaching a maximum value above 60% H_2O. RLS features at *ca.* 490 nm (Q visible bands) are also detectable in the spectrum. The strong intensities observed indicate the formation of large aggregates, typically 10^4–10^5 monomer units. (It has been reported that the minimum

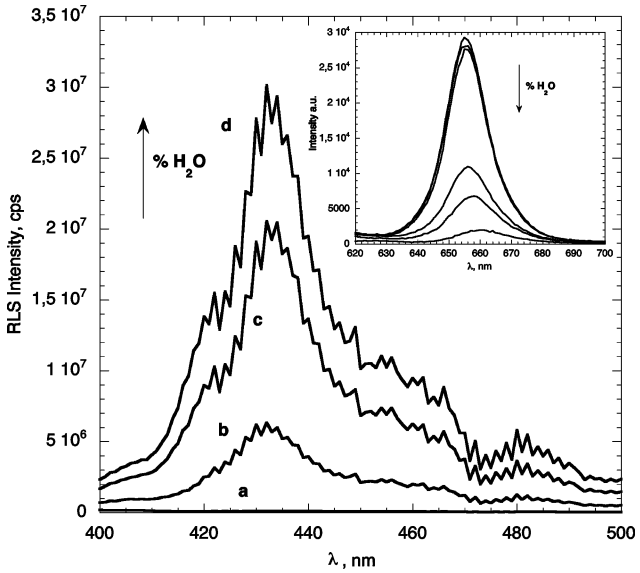

Fig. 3 RLS spectra of **2**, 1.1 μM in various MeCN–H_2O mixtures: (a) 0–35%, (b) 40%, (c) 45%, (d) 60% H_2O. Trace (a) appears at near zero on the plot. In the inset, the corresponding (a, top three traces)–(d) fluorescence emission spectra are reported. The arrows indicate the spectral changes upon increasing water proportion.

number of interacting chromophores needed to observe the RLS effect is $n \geq 25$. See, for example ref. 55) It is worth noting that the RLS spectra of porphyrin solutions in the monomeric form are undetectable on the observed intensity scale.

Analogous results are observed in the case of the bis-pentafluorophenyl derivative **7**, with the notable difference that this derivative shows, as expected, a maximum RLS effect at a somewhat higher water : MeCN ratio. Moreover, the relative RLS intensities, normalized by the relative molar extinction coefficients, are less pronounced (*ca.* 67%), probably indicating the formation of smaller aggregates.

Kinetic studies on the aggregation of title glycoporphyrins **2** and **7** have been performed in MeCN–H_2O solvent mixtures. The kinetics of aggregation can be carried out by conventional hand-mixing techniques, and can be conveniently followed by monitoring the decrease of Soret band intensity with time. In the case of porphyrin **2** the kinetic experiments have been carried out in a 1 : 1 MeCN–H_2O mixture. In the case of the "less hydrophobic" pentafluorophenyl derivative **7**, the aggregation occurs, as already evidenced in the preliminary solvent driven aggregation experiments (*vide supra*), only at higher water proportions (*i.e.*, ≥55%). At lower water contents no aggregation is observed, even after a prolonged time, as witnessed by the invariance of the UV-visible spectral pattern of the porphyrin solutions.

It has been reported[56] that the aggregation process can be quite dependent on either the initiation protocol, such as, for example, the mixing order of solution components, and on the ageing of the porphyrin stock solutions. In our case, using freshly prepared solutions and the same order of mixing ensures good reproducibility, as indicated in the Experimental section. However, different mixing protocols gave similar results, although of lower reproducibility, in terms of kinetic parameter values.

The experimental data points can be nicely fit by a so-called "stretched exponential" equation (eqn (1)).[57]

$$E = E_0 + \Delta E[1 - \exp(-(kt)^n)] \quad (1)$$

In this equation E_0 represents the initial extinction at $t = 0$, $\Delta E = E_\infty - E_0$ is the difference between the initial extinction value ($t = 0$) and that at $t = \infty$, k is the kinetic rate constant, and n is the aggregation growth factor, related to the mean value of binding sites available for aggregate growth process. This equation is valid in the case of monodispersed systems,[58] in which large clusters are formed by interaction between initial smaller clusters (seeds) and monomers. In this case, known as diffusion limited aggregation (DLA), the n factor is required to be <1. Notable examples are reported in the aggregation of charged cyanine dyes on charged polymeric templates, such as poly(vinylsulfonate).[48] A typical example is reported in Fig. 4, in which the close adherence of the experimental points to the calculated curve fit can be nicely evidenced. The quality of the fit is generally very good, with $R^2 \geq 0.9996$, and the calculated values for E_∞ and E_0 are always in excellent agreement with the experimental values. It is worth mentioning that aggregation kinetics followed by RLS spectroscopy gave similar results, in satisfactory agreement (Fig. 4, inset; Table 1). This clearly indicates that these two techniques are probing the same aggregation process.

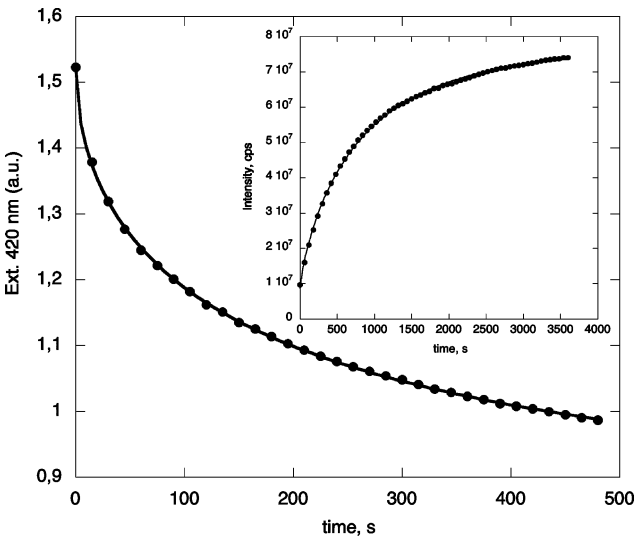

Fig. 4 Aggregation kinetics of **2** (3.7×10^{-6} M; MeCN–H_2O 50 : 50, UV-vis spectroscopy). The full circles are the experimental points and the continuous line represents the theoretical curve fit according to eqn (1). Inset: corresponding kinetic plot, followed by RLS (see text).

Table 1 Kinetic parameters of the aggregation reaction of **2** and **7** [a]

Entry	[P]/M	k_{agg} (**2**)/s^{-1} [b]	k_{agg} (**7**)/s^{-1} [c]
1	1.1×10^{-6}	1.3×10^{-3} (0.62)	1.0×10^{-3} (0.39)
2	2.2×10^{-6}	2.1×10^{-3} (0.60)	
3	3.7×10^{-6}	2.8×10^{-3} (0.64)	1.6×10^{-3} (0.42)
4	3.7×10^{-6}	2.7×10^{-3} (0.66)[d]	
5	3.7×10^{-6}	1.2×10^{-3} (0.76)[e]	
6	7.6×10^{-6}	5.4×10^{-3} (0.61)	2.4×10^{-3} (0.40)
7	1.1×10^{-5}	8.7×10^{-3} (0.67)	4.9×10^{-3} (0.45)

[a] $T = 298$ K. The value of parameter n is reported in parentheses (see text). Runs are in duplicate with uncertainties within 5%. [b] In MeCN–H_2O 50 : 50. [c] in MeCN–H_2O 45 : 55. [d] Protocol of preparation **B**. [e] Followed by RLS.

The results, in terms of apparent aggregation rate constant (k_{agg}, s^{-1}) and n values, are reported in Table 1. From inspection of the table, it is evident that an increase of aggregation rate is promoted by increasing the initial porphyrin concentration. The porphyrin derivative **2** shows a higher rate of aggregation with respect to the counterpart **7**. This, again, can be related to the different peripheral substitution pattern. This would infer a different hydrophobicity of the macrocycles, producing a different tendency to self-aggregation. Apparently, the more electron-withdrawing C_6F_5 moiety promotes a more favorable solvation, resulting in a slower aggregation rate. The effect of the different structural parameters reflects itself also in the mean n values. The above kinetic studies gave mean values of 0.63 and 0.42, for **2** and **7**, respectively. Moreover, they are virtually independent, within the experimental uncertainties, of the initial substrate concentration, safely ruling out a change in aggregation mechanism upon varying substrate concentration. Again, the differences found for the values of n, although at the present stage of unstraightforward interpretation, would be certainly related to the different structural features. Addressed studies will be carried out to elucidate this topic, and the results will be reported elsewhere.

Aggregation experiments, conducted at different ionic strengths, have been further carried out in the case of both **2** and **7** derivatives, and the results, in terms of aggregation constant values (k_{agg}) and parameter n, are reported in Table 2, and in graphical form in Fig. 5.

The increase of ionic strength of the bulk medium (NaBr addition) promotes an increase of the aggregation rate, as it would be expected for a self-interaction mainly promoted by the solvophobic effect.[59] Interestingly, the effect of the medium is quite similar for the two derivatives, ruling out the occurrence of a specific interaction of the ions with the polar porphyrin frames (Fig. 6).

Remarkably, the n values remain unchanged, within experimental error, with respect to the values obtained in the case of aggregation carried out in the absence of NaBr. This finding would safely rule out a change in the aggregation mechanism. In different case of aggregation of charged, water soluble, porphyrin derivatives, namely tetrakis(sulfonatophenyl)porphine,[60] the addition of salts causes a change of mechanism, from DLA to DCCLA (diffusion limited cluster–cluster aggregation). This effect has been interpreted on the basis of specific ion-pairing (cation–anionic porphine) interaction. In our present case (*i.e.*, uncharged species), the addition of salts results in an aspecific, general salt effect, which apparently influences only the rate of self-interaction.

Table 2 Kinetic parameters of the aggregation reaction of **2** and **7** in the presence of NaBr[a]

Entry	[NaBr]/M	k_{agg} (**2**)/s^{-1}[b]	k_{agg} (**7**)/s^{-1}[c]
1	0.0020	0.0041 (0.61)	0.0045 (0.43)
2	0.010	0.0087 (0.68)	1.2×10^{-2} (0.39)
3	0.010	0.0090 (0.70)[d]	
4	0.050	0.026 (0.63)	0.032 (0.42)
5	0.10	0.040 (0.67)	0.044 (0.46)
6	1.0	[e]	[e]

[a] [P] = 3.7×10^{-6} M; T = 298 K. In parentheses the value of parameter n is reported (see text). Runs are in duplicate with uncertainties within 5%. [b] In MeCN–H_2O 50 : 50. [c] in MeCN–H_2O 45 : 55. [d] Protocol of preparation **B**. [e] Too fast to be measured.

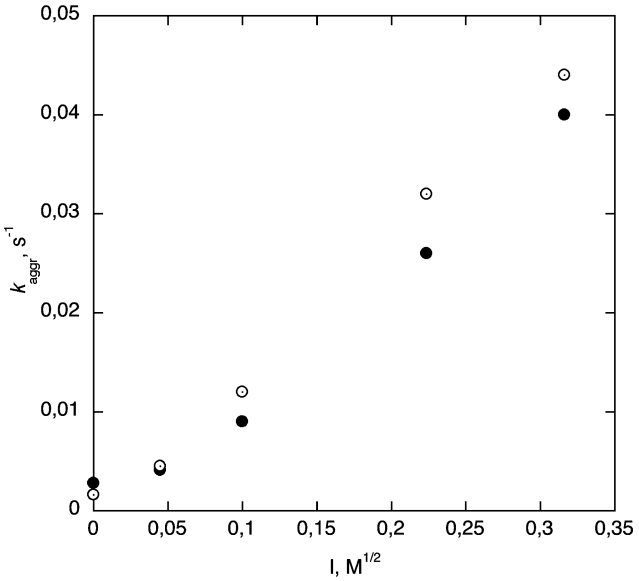

Fig. 5 Kinetic constant values of **7** (○) and 2 (●) (7.3×10^{-6} M; MeCN–H_2O 50 : 50) as a function of ionic strength.

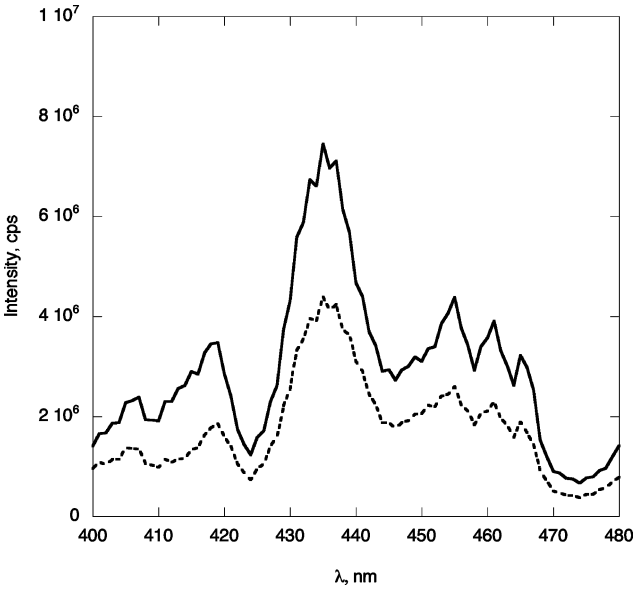

Fig. 6 RLS spectra of **2** (3.7 μM in 50% aqueous MeCN, T = 298 K). Full line: [NaBr] = 0.0 M; dashed line: [NaBr] = 0.010 M.

At a salt concentration higher than 0.1 M, the aggregation became too rapid to be followed by conventional techniques. Remarkably, in those latter cases, the aggregation results in an evident opalescence of the solution. This is accompanied by dramatic spectral changes, in which the absorption bands are severely broadened, with non-zero extinction throughout the visible range. Moreover, an anomalous B : Q band intensity ratio is observed (see Fig. 7). This phenomenon is similar to that recently reported in the case of formation of spermine-induced porphyrin fractal J-aggregation, in which this unusual enhancement of light scattering has been attributed to the formation of large porphyrin aggregates behaving as metal particles.[61]

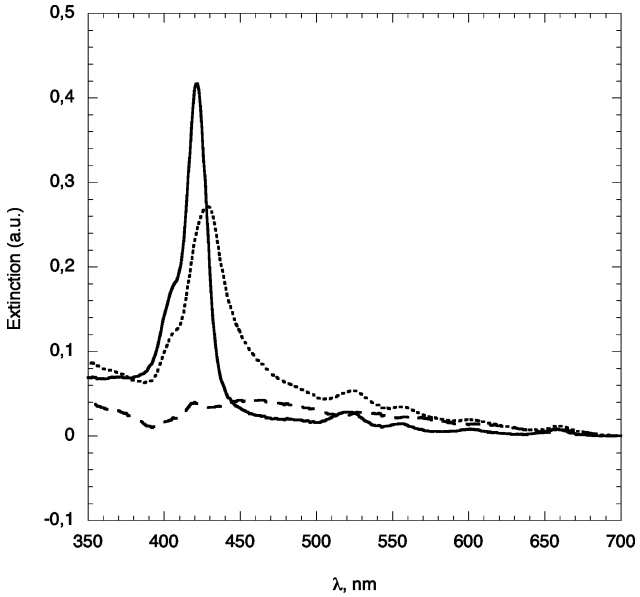

Fig. 7 UV-visible spectra of **2** in MeCN (solid line); in MeCN–H_2O [NaBr] = 0.0 M (dotted line) and in MeCN–H_2O [NaBr] = 1.0 M (dashed line).

RLS spectra of **2** and **7** (3.7 μM; 50% aqueous MeCN or 45% aqueous MeCN, respectively) show a reduction in scattering intensities (Fig. 8), once performed in the presence of added salt (NaBr, 0.010 M). This would indicate, in the first instance, that the higher ionic strength, although promoting a faster aggregation, results in self-assembled species characterised by a lower size (lower number of components). This could be tentatively explained in terms of a fine balance between two opposing effects, *i.e.*, (i) a general increase of the polarity of the bulk medium boosting a faster aggregation by π–π interaction (hydrophobic effect) and, concomitantly, (ii) the onset of electrostatic repulsion between the Na^+ ions that surround the polar appended functionalities on the

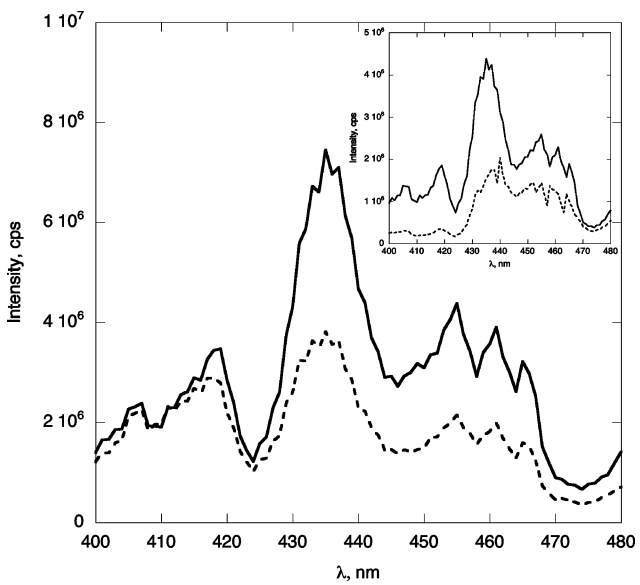

Fig. 8 RLS spectra of **2** and **7** (inset) (3.7 μM in 50% aqueous MeCN, T = 298 K) at [NaBr] = 0.0 M (solid line) and [NaBr] = 0.010 M (dotted line).

tetrapyrrolic frames. This latter effect would become predominant on increasing the size of the porphyrin aggregates.

Circular dichroism (CD) spectroscopy has been found to be an excellent tool for the studies of porphyrin chiral aggregates. The formation of chiral aggregates has been achieved by several means. Seminal papers by Pasternack demonstrated the formation of chiral porphyrin aggregates by templating with DNA, RNA, or other chiral synthetic polymers.[62] Supramolecular chirogenesis can be induced in achiral porphyrin systems by metal coordination.[63] Spontaneous chiral symmetry breaking has been achieved by stirring effects in homoassociation of water soluble derivatives.[64]

We recently reported[47] that the presence of a chiral functionality on the molecular frame of amphiphilic porphyrin derivatives steers the aggregation toward the formation of supramolecular structures featuring supramolecular chirality. In light of the above reports, the study of the aggregation of these title glyco-derivatives certainly constitutes an intriguing task, not only from an academic point of view, but also for practical, future applications.

CD experiments, carried out on porphyrins **2** and **7**, reveal that the aggregation results in the formation of intrinsically-chiral assemblies, triggered by the presence of the sugar moieties (Fig. 9). The aggregation results, in both of the cases, in a strong, negative bisignate CD spectrum, indicating that the electronically-coupled macrocycles are held in a mutual chiral conformation.

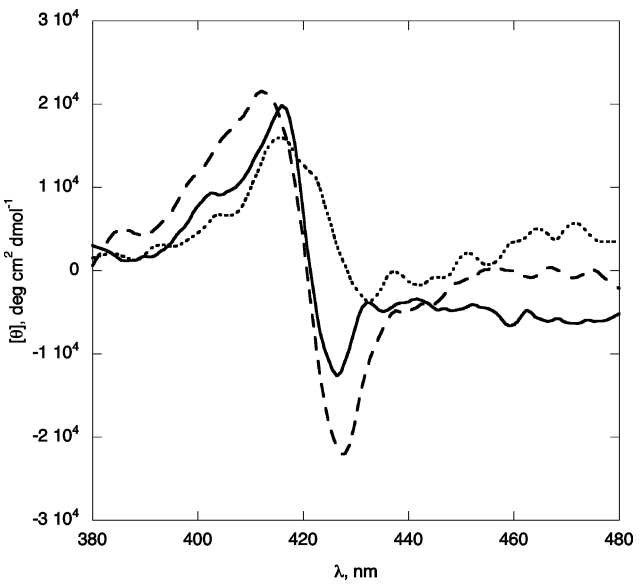

Fig. 9 CD spectra of porphyrins (3.7 μM) in aggregative conditions. (Solid line) **2** in H_2O–MeCN 1 : 1; (dashed line) **7** in H_2O–MeCN 55 : 45; (dotted line) **7** H_2O–MeCN 55 : 45, NaBr 0.010 M.

Remarkably, some differences in the CD spectral features can be evidenced. Porphyrin **2** (solid line) give rise to a negative peak at λ 426 nm ($[\theta] = -1.2 \times 10^4$) and a positive one at λ 416 nm ($[\theta] = +2.0 \times 10^4$), with the "zero point" at 420 nm, whereas **7** aggregates present slightly shifted and somewhat more intense spectral features with λ 427 nm ($[\theta] = -2.3 \times 10^4$) and λ 412 nm ($[\theta] = +2.2 \times 10^4$), with the "zero point" at 420 nm (dashed line). The stronger intensity of the spectral CD features of **7** should indicate the formation of porphyrin assemblies, although of smaller size (RLS experiments), which are characterized by a higher degree of asymmetry. Further important insights can

be given by monitoring the evolution of CD signals during the aggregation process. In both the cases of porphyrin **2** and **7**, the maximum CD intensity is reached during the very first part of the process (*i.e.*, within few minutes from solution preparation and mixing), reaching a steady value after this initial period. This, according to the proposed mechanism of aggregation (DLA), would imply the fast formation of initial chiral smaller cluster, slowly growing in size, with no further modification of the whole chirality, during the subsequent growth, which is completed, in the same experimental condition, within one–two hours after mixing (UV-visible and RLS experiments).

Interestingly, the aggregation promoted in the presence of NaBr (0.01 M) resulted in the formation of porphyrin suprastructures characterised by a lower degree of asymmetry, as evidenced by the lower intensities of relative CD spectral features (dotted line, Fig. 9). This would indicate the formation of aggregates characterized by a lower degree of supramolecular chirality. Moreover, in the case of aggregation of **2**, scarcely detectable CD signals are obtained. The different CD intensities can be ascribed to a different porphyrin–porphyrin geometrical orientation. It has been stated, for the aggregation of related tetrapyrrolic macrocycles, that the intensity of the CD signals are directly related to the intrinsic asymmetry of the system, and not on the size of the growing structures.[65] In earlier cases, reported by Pasternack *et al.*, the formation of highly charged, water soluble, porphyrin–DNA assemblies, occurred with dramatic variation of CD features (sign inversion) upon changing the ionic strength of the medium.[66] This has been attributed to a change of conformation from a "face-on" to "end-on" orientation of the aggregates. In our case this effect, although not as great as the above reported, concerning the aggregation between uncharged platforms, would be explained in terms of the shielding effect of the Na^+ with the polar groups (Na^+- - -:OR; Na^+- - -:F_5C_6– ion–dipole interaction), that would result in a less effective reading of the molecular information stored in the stereogenic centers during the molecular recognition process.

All these findings would indicate the possibility of some tuning and control of the final structural morphology and the electronic properties of the investigated aggregates. (For a recent report on the modulation of the tuning of supramolecular chirality of self-assembled porphyrin systems by solvent modulation of π–π stacking interactions, see ref. 67.) We recently reported a similar behaviour (*cf.* ref. 47*a*) in the case of solvent driven aggregation of amphiphilic chiral porphyrin derivatives. These results can be of great importance in many areas of research, such as, for example, the construction of artificial light-harvesting systems (for some recent examples see ref. 68), supramolecular materials,[69] optoelectronic devices,[70] and for the development of stereoselective solid-state sensors, in which the chiral features of the receptors are of crucial importance to chiral molecular recognition and discrimination.[71]

Experimental

TLC was performed on HF_{254} plates (Merck), detection by UV light or by spraying with a solution of 5 g of $Ce(SO_4)_2(H_2O)_4$ in 500 ml 10% H_2SO_4 and subsequent heating. Flash column chromatography was performed on silica gel (MERCK, 100–160 μm) in solvents, distilled prior to use. Optical rotations were measured in chloroform solutions on a Rudolph Research Autopol IV polarimeter at 25 °C and $[a]_D$ values are given in 10^{-1} deg cm^2 g^{-1} with concentration in 10 g l^{-1}. Routine UV spectra were recorded on Varian Cary 50 UV-VIS spectrometer; wavelengths are given in nm; molar absorptivity (ε) is given in parentheses, in m^2 mol^{-1}. IR spectra (wavenumbers in cm $^{-1}$) were recorded on a Perkin-Elmer PE 580 spectrometer in $CHCl_3$ solutions (temperature 23 °C), unless stated otherwise. ^{1}H and ^{13}C NMR spectra were taken in deuterochloroform (Aldrich, 99.8% D) on a Bruker AVANCE 500 (500.1 MHz for ^{1}H and 125.8 MHz for ^{13}C) FT NMR spectrometer at 300 K if not stated otherwise. As standard, the internal signal of tetramethylsilane (δ 0.0) for ^{1}H and central line of solvent (δ 77.0) for ^{13}C spectra were used. Chemical shifts are presented in ppm (δ), coupling constants in Hz (J). Mass spectra were taken on a Q TOF micromass spectrometer with direct inlet (ESI) or on a ZAB-EQ (VG Analytical) instrument (FAB) with Xe ionization, accelerating voltage 8 kV. Microanalysis was performed on an elemental analyzer Perkin-Elmer 2400 Series II CHNS/O.

All solvents used were of the highest degree of purity and used as received. Porphyrin solutions for spectroscopic studies have been prepared by using solvents of spectroscopic grade. Milli-Q, Millipore, previously doubly distilled water, was used for the preparation of porphyrin aqueous solutions.

Kinetic studies

Kinetic experiments were performed on a Perkin Elmer λ18 spectrophotometer equipped with a thermostating apparatus, by measuring the UV-visible spectroscopic changes (Soret B band) of porphyrin derivatives with time. Porphyrin aqueous solutions, suited for kinetic studies, were prepared as follows (protocol **A**). Proper aliquots, of a millimolar stock solution in acetonitrile (15 150 μL), were added to 2.0 mL of acetonitrile in an 8 mL glass vial. To this solution, 2.0 mL of water were then added and the resulting solution was vigorously shaken. A 3 mL portion was then transferred in a quartz cuvette and the relative UV-visible spectra acquired. This procedure ensures a 50 : 50 H_2O–MeCN (v/v) final solvent composition, with final porphyrin concentrations spanning the range of 1.1 to 11.1 × 10^{-6} M. Values of k were obtained by analysing the absorbance (extinction) *vs.* time data points by a nonconventional kinetic treatment, earlier proposed by Pasternack for a related case of the aggregation of porphyrin derivatives on (bio)polymer templates.

The equation used is as follows:

$$E = E_0 + (E_{inf} - E_0)[1 - \exp(-(kt)^n)] \quad (2)$$

where E, E_0, E_{inf} are the extinction values at time t, initially, and at equilibrium, respectively. The kinetic parameters, k and n, where obtained by nonlinear least-squares regression fit (Kaleidagraph® program, Synergy Software, 2003) over hundreds of experimental data points. Values obtained at different wavelengths (*e.g.*, 450 nm) were similar, within experimental errors. Data reported are the average values of at least two different runs.

A different protocol, entailing the simple addition of porphyrin stock solution to a preformed H_2O–MeCN mixture (protocol **B**) gave, although with a lower degree of reproducibility, similar results. Attempts to perform kinetic runs at higher H_2O–MeCN solvent composition by standard routine equipment failed, as the spectral pattern changes were too rapid to be conveniently

followed. Studies by rapid-mixing methods are planned, and the results will be reported elsewhere.

Analogous experimental protocols have been used in the case of kinetic experiments run in the presence of NaBr. Proper aliquots of a millimolar stock solution in acetonitrile (50 μL), where added to a 2.0 mL of acetonitrile in an 8 mL glass vial. To this solution 2.0 mL of NaBr solution in water were then added and the resulting solution vigorously shaken and transferred in a quartz cuvette and the relative UV-visible spectra acquired.

CD spectroscopic studies

CD spectra have been performed on a JASCO J-600, equipped with a thermostatted cell holder, and purged with ultra-pure nitrogen gas.

Resonance light scattering experiments

RLS experiments have been performed on a Spex Fluorolog Fluorimeter. Spectra have been acquired, at 25 ± 0.5 °C, in a "synchronous scan" mode, in which the emission and excitation monochromators are pre-set to identical wavelengths. Solutions have been prepared by following the protocol used in the kinetic experiments (protocol **A**).

Fluorescence spectroscopy experiments

Fluorescence, excitation spectra were recorded, at 25 ± 0.5 °C, on a Spex Fluorolog Fluorimeter.

5,10,15,20-Tetrakis(2,3,4,6-tetra-*O*-benzyl-α-D-galactopyranosylmethyl)porphyrin (2). Through the solution of pyrrole (33 μl, 0.48 mmol) and aldehyde **1** (ref. 40, 275 mg, 0.49 mmol) in 40 ml of dry dichloromethane Ar was bubbled for 10 min. Then 6 μl of $BF_3{\cdot}Et_2O$ was added as catalyst. The reaction vessel was shielded from light and stirring under Ar at ambient temperature was continued for 3 hours. Then, the reaction mixture was transferred *via* canula into another flask with 118 mg of DDQ, and the reaction mixture was stirred at room temperature for an additional 12 hours. After this period silica gel was added and the solvent was evaporated under vacuum.

The resulting powder was placed at the top of a short silica gel column. Increasing polarity elution with light petroleum–ethyl acetate 4 : 1 gave porphyrin **2** (55 mg, 18%) as a dark brown–violet amorphous solid. $[a]^{25}$ (c 9 × 10^{-3}) $[a]_{436}$ = +910; $[a]_{546}$ = +489; $[a]_D$ = +311; $[a]_{633}$ = +311. For $C_{160}H_{158}N_4O_{20}$ (2456.9) calculated: 78.21% C, 2.28% N; 6.48% H, found: 77.95% C, 2.02% N, 6.07% H.

5,10,15,20-Tetrakis(2,3,4,6-tetra-*O*-benzyl-α-D-glucopyranosylmethyl)porphyrin (4). Through the solution of pyrrole (36 μl, 0.52 mmol) and aldehyde **3** (ref. 41, 300 mg, 0.53 mmol) in 43 ml of dry dichloromethane Ar was bubbled for 10 min. Then 7 μl of $BF_3{\cdot}Et_2O$ was added as catalyst. The reaction vessel was shielded from light and stirring under Ar at ambient temperature was continued for 2 hours. Then, the reaction mixture was transferred *via* canula into another flask with 128 mg of DDQ, and the reaction mixture was stirred at room temperature for an additional 12 hours. After this period silica gel was added and the solvent was evaporated under vacuum.

The resulting powder was placed at the top of a short silica gel column. Increasing polarity elution with light petroleum, light petroleum–ethyl acetate 4 : 1 gave porphyrin **4** (120 mg, 36%) as a dark brown–violet solid. $[a]^{25}$ (c 2.8 × 10^{-3}) $[a]_{436}$ = +720; $[a]_{546}$ = +267; $[a]_D$ = +167; $[a]_{633}$ = +133. For $C_{160}H_{158}N_4O_{20}$ (2456.9) calculated: 78.21% C, 2.28% N; 6.48% H, found: 77.84% C, 2.24% H, 5.95% N.

2,6-Anhydro-1,3,4,5-tetra-*O*-benzyl-7,8-dideoxy-8,8-di-1*H*-pyrrol-2-yl-D-*glycero*-L-*galacto*-octitol (5). Through the solution of pyrrole (0.68 ml, 9.8 mmol) and aldehyde **1** (ref. 40, 270 mg, 0.48 mmol) in 16.2 ml of dry dichloromethane Ar was bubbled for 10 min. Then 55 μl of TFA was added and a solution was stirred in the dark at ambient temperature under Ar for 90 min. The reaction was quenched by addition of a saturated aqueous solution of $NaHCO_3$ and solid NH_4Cl.

The mixture was extracted with diethylether and the combined organic layers were dried $MgSO_4$, filtered and concentrated under vacuum. The crude product was purified by flash chromatography (light petroleum–ethyl acetate 12 : 1) to give 160 mg (49%) of dipyrrylmethane **5** as a dark brown solid. $[a]^{25}$ (c 5.6 × 10^{-3}) $[a]_{365}$ = −300; $[a]_{405}$ = −200; $[a]_{436}$ = −183; $[a]_{546}$ = −67; $[a]_D$ = −50; $[a]_{365}$ = −50. For $C_{44}H_{46}N_2O_5$ (682.8) calculated: 77.39% C, 6.79% H, 4.10% N; found: 76.98% C, 6.45% H, 3.61% N.

2,6-Anhydro-1,3,4,5-tetra-*O*-benzyl-7,8-dideoxy-8,8-di-1*H*-pyrrol-2-yl-D-*glycero*-L-*gulo*-octitol (6). Through the solution of pyrrole (2.5 ml, 36.0 mmol) and aldehyde **3** (ref. 41, 640 mg, 1.13 mmol) in 15 ml of dry dichloromethane Ar was bubbled for 10 min. Then 50 μl of TFA was added and a solution was stirred in the dark at ambient temperature under Ar for 110 min. The reaction was quenched by addition of a saturated aqueous solution of $NaHCO_3$ and solid NH_4Cl.

The mixture was extracted with diethylether and the combined organic layers were dried $MgSO_4$, filtered and concentrated under vacuum. The crude product was purified by flash chromatography (hexane–ethyl acetate 12 : 1) to give 650 mg (84%) of dipyrrylmethane **6** as a pale violet foam. $[a]^{25}$ (c 5 × 10^{-3}) $[a]_{365}$ = −250; $[a]_{405}$ = −148; $[a]_{436}$ = −110; $[a]_{546}$ = −67; $[a]_D$ = −30; $[a]_{365}$ = −30. For $C_{44}H_{46}N_2O_5$ (682.8) calculated: 77.39% C, 6.79% H, 4.10% N; found: 76.99% C, 6.54% H, 3.59% N.

5,15-[Bis(pentafluorophenyl)]-10,20-[bis-(2,3,4,6-tetra-*O*-benzyl-α-D-galactopyranosylmethyl)porphyrin 7. (i) To a solution of dipyrrylmethane **5** (130 mg, 0.19 mmol) in 40 ml of dry dichloromethane was added a solution of pentafluorobenzaldehyde (37 mg, 0.19 mmol) in 0.5 ml of dry dichloromethane *via* canula. Then Ar was bubbled through the reaction mixture for 10 min. Then TFA (18 μl, 0.19 mmol) was added as catalyst. The reaction vessel was shielded from light and stirring was continued for 20 hours under Ar at ambient temperature. Then the triethylamine (26 μl, 0.19 mmol) and DDQ (90.8 mg, 0.4 mmol) were added and the reaction mixture was stirred at room temperature for an additional 2 hours.

After this period, silica gel was added and the solvent was evaporated under vacuum. The resulting powder was placed at the top of a short silica gel column. Increasing polarity elution with light petroleum, light petroleum–ethyl acetate 4 : 1 gave porphyrin **7** (37 mg, 22%) as a dark brown–violet amorphous solid. $[a]^{25}$ (c 3.8 × 10^{-3}) $[a]_{436}$ = −27 730; $[a]_{546}$ = −16 798; $[a]_D$ = −14 132; $[a]_{633}$ = −13 332 For $C_{102}H_{84}F_{10}N_4O_{10}$ (1715.7) calculated: 71.40% C, 4.93% H, 3.27% N, 11.07; found: 71.74% C, 5.48% H, 2.60% N.

(ii) To a solution of dipyrrylmethane **9** (100 mg, 0.32 mmol) (ref. 44) in 67 ml of dry dichloromethane was added a solution of aldehyde **1** (182 mg, 0.32 mmol) in 0.5 ml of dry dichloromethane *via* canula then Ar was bubbled though the reaction mixture for 10 min. Then TFA (31 µl, 0.32 mmol) was added as catalyst. The reaction vessel was shielded from light and stirring under Ar at ambient temperature was continued for 20 hours. Then the triethylamine (44 µl, 0.32 mmol) and DDQ (152 mg, 0.67 mmol) were added and the reaction mixture was stirred at room temperature for an additional 3 hours. After this period silica gel was added and the solvent was evaporated under vacuum. The resulting powder was placed at the top of a short silica gel column. Increasing polarity elution with light petroleum, light petroleum–ethyl acetate 4 : 1 gave porphyrin **7** (73 mg, 27%) as dark brown–violet solid of the same properties as had (i).

5,15-[Bis(pentafluorophenyl)]-10,20-[bis-(α-D-galactopyranosylmethyl)porphyrin (10). To a solution of porphyrin **7** (100 mg, 0.058 mmol) in CH_2Cl_2 1 ml and MeOH 2 ml 10% Pd(C) 90 mg was added. The reaction mixture was stirred under H_2 (atmospheric pressure) at ambient temperature for one night. After filtration, silica gel was added and solvents were evaporated under reduced pressure. The resulting powder was placed at the top of a short silica gel column. Increasing polarity elution with $CHCl_3$, $CHCl_3$–MeOH 2 : 1 gave porphyrin **10** (37 mg, 63%) as dark green amorphous solid.

UV (MeOH) λ_{max} 410 (54600); 510 (5180); 543 (2340); 589 (1950); 647 (1970). ^{1}H NMR 300 MHz (CD_3OD): porphyrin moiety −9.90 bs (4H), 9.05 bs (4H); sugar moiety −4.05–3.52 m (18H). ^{13}C NMR 75 MHz (CD_3OD): 151.17, 149.11, 145.19, 141.17, 137.73, 133.72, 129.79, 129.66, 71.51.71.12, 70.89, 70.67, 70.55, 70.21, 69.97, 37.76. For $C_{46}H_{36}F_{10}N_4O_{10}$ (exact mass 994.23) MS (*m*/*z*, FAB): 995.0 $(M + H)^+$, 1011.1 $(M + H_2O)^+$.

Acknowledgements

This work was supported by the Ministry of Education, Youth and Sports of the Czech Republic, with projects no. MSM6046137305 (LK), 203/06/0006 (PD), 1P04OCD31.001 (MD), 2B06024-SUPRAFYT of the National Research Program II (JM), and was a part of project Z4 055 0506 (DS, PS). We are indebted to Dr P. Fiedler for taking and interpretation of IR spectra. Mass spectra were measured by the Mass Spectroscopy Laboratory of the IOCB (Dr K. Ubik, Head), elemental analyses were done by the Analytical Department of the IOCB (Dr L. Váchová, head).

References

1 J.-M. Lehn, *Angew. Chem., Int. Ed. Engl.*, 1988, **27**, 89–112.
2 N. Aubert, V. Troiani, M. Gross and N. Solladie, *Tetrahedron Lett.*, 2002, **43**, 8405–8408.
3 O. Rusin, M. Hub and V. Král, *Mater. Sci. Eng., C*, 2001, **C18**, 135–140.
4 J. Charvátová, O. Rusin, V. Král, K. Volka and P. Matějka, *Sens. Actuators, B*, 2001, **B76**, 366–372.
5 N. Solladie, M. Gross, J.-P. Gisselbrecht and C. Sooambar, *Chem. Commun.*, 2001, **21**, 2206–2207.
6 D. Gabel, S. Harfst, D. Moller, H. Ketz, T. Peymann and J. Roesler, *Current Topics in the Chemistry of Boron*, 1994, RSC, London, UK, pp. 161–164; D. Gabel, S. Harfst, D. Moller, H. Ketz, T. Peymann and J. Roesler, *Chem. Abs.*, 1995, **122**, 31777.
7 X. Chen, L. Hui, D. A. Foster and C. M. Drain, *Biochemistry*, 2004, **43**, 10918–10929.
8 X. Chen, L. Hui, D. A. Foster and C. M. Drain, *Abs. Pap., 227th Am. Chem. Soc. National Meeting*, Anaheim, CA, United States, March 28–April 1, 2004.
9 D. Gierson, P. Maillard, B. Loock, T. Figueiredo and D. Carrez, *Eur. Pat.* 1279676, 2003; D. Gierson, P. Maillard, B. Loock, T. Figueiredo and D. Carrez, *Chem. Abs.*, 2003, **138**, 119353.
10 S. Yano, *J. Photosci.*, 2002, **9**, 174–177.
11 Y. Mikata, Y. Onchi, K. Tabata, S.-I. Ogura, I. Okura, H. Ono and S. Yano, *Tetrahedron Lett.*, 1998, **39**, 4505–4508.
12 N. Ono, M. Bougauchi and K. Maruyama, *Tetrahedron Lett.*, 1992, **33**, 1629–1632.
13 Z. Li, K. Wang, X. Zhu and Z. Yi, *Wuhan Univ. J. Nat. Sci.*, 2002, **7**, 350–352, (*Chem. Abs.*, 2003, **139**, 164929).
14 A. Bourhim, O. Gaud, R. Granet, P. Krausz and M. Spiro, *SYNLETT*, 1993, **8**, 563–564.
15 A. F. Mironov, G. M. Isaeva, V. I. Shvets, R. P. Evstigneeva, A. N. Stepanov, A. A. Perov and S. E. Kupriyanov, *Bioorg. Khim.*, 1978, **4**, 1410–1413.
16 M. Momenteau, P. Maillard, M.-A. De Belinay, D. Carrez and A. Croisy, *J. Biomed. Opt.*, 1999, **4**, 298–318.
17 M. Dukh, D. Šaman, K. Lang, V. Pouzar, I. Černý, P. Drašar and V. Král, *Org. Biomol. Chem.*, 2003, **1**, 3458–3463.
18 K. Zelenka, T. Trnka, I. Tišlerová, V. Král, M. Dukh and P. Drašar, *Collect. Czech. Chem. Commun.*, 2004, **69**, 1149–1160.
19 M. Dukh, P. Drašar, I. Černý, V. Pouzar, J. A. Shriver, V. Král and J. L. Sessler, *Supramol. Chem.*, 2002, **14**, 237–244.
20 X. Chen and C. M. Drain, *Drug Des. Rev.—Online*, 2004, **1**, 215–234.
21 C. Schell and H. K. Hombrecher, *Chem.–Eur. J.*, 1999, 587–598.
22 M. Sirish and H.-J. Schneider, *Chem. Commun.*, 2000, 23–24.
23 X.-B. Zhang, C.-C. Guo, S.-H. Chen, G.-L. Shen and R.-Q. Yu, *Fresenius' J. Anal. Chem.*, 2001, **369**, 422–427.
24 P. Maillard, J. L. Guerquin-Kern and M. Momenteau, *Tetrahedron Lett.*, 1991, **32**, 4901–4904.
25 S. VilainDeshayes, A. Robert, P. Maillard, B. Meunier and M. Momenteau, *J. Mol. Catal. A: Chem.*, 1996, **113**, 23–34.
26 S. VilainDeshayes, P. Maillard and M. Momenteau, *J. Mol. Catal. A: Chem.*, 1996, 201–208.
27 S. Vilain, P. Maillard and M. Momenteau, *J. Chem. Soc., Chem. Commun.*, 1994, 1697–1698.
28 M. Spiro, J. C. Blais, G. Bolbach, F. Fournier, J. C. Tabet, K. Driaf, O. Gaud, R. Granet and P. Krausz, *Int. J. Mass Spectrom. Ion Processes*, 1994, **134**, 229–238.
29 K. Kohata, H. Higashio, Y. Yamaguchi, M. Koketsu and T. Odashima, *Bull. Chem. Soc. Jpn.*, 1994, **67**, 668–679.
30 M. Dukh, D. Šaman, J. Kroulík, I. Černý, V. Pouzar, V. Král and P. Drašar, *Tetrahedron*, 2003, **59**, 4069–4076.
31 P. Drašar, M. Buděšínský, M. Reschel, V. Pouzar and I. Černý, *Steroids*, 2005, **70**, 615–625.
32 M. Cornia, M. Menozzi, E. Ragg, S. Mazzini, A. Scarafoni, F. Zanardi and G. Casiraghi, *Tetrahedron*, 2000, **56**, 3977–3983.
33 P. Maillard, C. Huel and M. Momenteau, *Tetrahedron Lett.*, 1992, **33**, 8081–8084.
34 G. Casiraghi, M. Cornia, F. Zanardi, G. Rassu, E. Ragg and R. Bortolini, *J. Org. Chem.*, 1994, **59**, 1801–1808.
35 R. Fiammengo, M. Crego-Calama, P. Timmerman and D. N. Reinhoudt, *Chem.–Eur. J.*, 2003, **9**, 784–792, and references therein.
36 *Carbohydrate Mimics: Concepts & Methods*, Y. Chapleur ed., Wiley-VCH Verlag GmbH, Weinheim, DE, 1998.
37 A. Sajida, E. Davoust, H. Savoie, N. A. Boa and W. R. Boyle, *Tetrahedron Lett.*, 2004, **45**, 6045–6047.
38 J. H. Fuhrhop, C. Demoulin, C. Boettcher, J. Konig and U. Siggel, *J. Am. Chem. Soc.*, 1992, **114**, 4159–4165.
39 P. Pasetto, X. Chen, Ch. M. Drain and R. W. Franck, *Chem. Commun.*, 2001, 507.
40 Z. Wang, H. Shao, E. Lacroix Wu, H. J. Jennings and W. Zou, *J. Org. Chem.*, 2003, **68**, 8097–8105.
41 E. Brema, C. Fungati, P. Grasselli, S. Serra and S. Zambotti, *Chem.–Eur. J.*, 2002, **8**, 1872–1878.
42 C. H. Lee and J. S. Lindsey, *Tetrahedron*, 1994, **50**, 11427–11440.
43 B. J. Littler, Y. Ciringh and J. S. Lindsey, *J. Org. Chem.*, 1999, **64**, 2864–2872.
44 H.-A. Wagenknecht, C. Claude and W.-D. Woggon, *Helv. Chim. Acta*, 1998, **81**, 1506–1520.
45 T. S. Balaban, M. Linke-Schaetzel, A. D. Bhise, N. Vanthuyne, C. Roussel, C. E. Anson, G. Buth, A. Eichhhöfer, K. Foster, D. Garab,

H. Gliemann, R. Goddard, T. Javorfi, A. K. Powell, H. Rösner and T. Schimmel, *Chem.–Eur. J.*, 2005, **11**, 2267–2275.
46 L. S. Dolci, E. Marzocchi, M. Montalti, L. Prodi, D. Monti, C. Di Natale, A. D'Amico and R. Paolesse, *Biosens. Bioelectron.*, 2006, **22**, 399–404.
47 (*a*) D. Monti, M. Venanzi, M. Mancini, C. Di Natale and R. Paolesse, *Chem. Commun.*, 2005, 2471–2473; (*b*) D. Monti, V. Cantonetti, M. Venanzi, C. Bombelli, F. Ceccacci and G. Mancini, *Chem. Commun.*, 2004, 972–973.
48 K. Zelenka, T. Trnka, P. Štěpánek, D. Monti, G. Mancini and P. Drašar, *2nd Workshop of COST D31 Action*, Tuscollana Frascati (IT), December 15–18, 2005.
49 M. Gouterman, *Optical Spectra and Electronic Structure of Porphyrins and Related Rings, in The Porphyrins, Vol. 3, Physical Chemistry, Part A.*, ed. D. Dolphin, Academic Press, New York, 1978.
50 (*a*) J. M. Ribò, J. M. Bofill, J. Crusats and R. Rubires, *Chem.–Eur. J.*, 2001, **7**, 2733–2737; (*b*) S. Okada and H. Segawa, *J. Am. Chem. Soc.*, 2003, **125**, 2792–2796.
51 N. Micali, F. Mallamace, M. Castriciano, A. Romeo and L. Monsù Scolaro, *Anal. Chem.*, 2001, **73**, 4958–4963.
52 (*a*) C. Shell and H. K. Hombrecher, *Chem.–Eur. J.*, 1999, **5**, 587–598; (*b*) D. Monti, A. Pastorini, M. Venanzi, S. Borocci and G. Mancini, *J. Porphyrins Phthalocyanines*, 2003, **7**, 181–190.
53 J. H. van Esch, M. C. Feiters, A. M. Peters and R. J. M. Nolte, *J. Phys. Chem.*, 1994, **98**, 5541–5551.
54 (*a*) R. F. Pasternack and P. J. Collings, *Science*, 1995, **269**, 935–939; (*b*) R. F. Pasternack, C. Bustamante, P. J. Collings, A. Giannetto and E. J. Gibbs, *J. Am. Chem. Soc.*, 1993, **115**, 5393–9539; (*c*) J. Parkash, J. H. Robblee, J. Agnew, E. Gibbs, P. Collings, R. F. Pasternack and J. C. de Paula, *Biophys. J.*, 1998, **74**, 2089–2099.
55 (*a*) P. A. J. de Witte, M. Castriciano, J. J. L. M. Cornelissen, L. Monsù Scolaro, R. J. M. Nolte and A. E. Rowan, *Chem.–Eur. J.*, 2002, **9**, 1775–1781; (*b*) P. Kubát, K. Lang, K. Procházková and P. Anzenbacher, Jr., *Langmuir*, 2003, **19**, 422–428.
56 R. F. Pastenack, C. Fleming, S. Herring, P. J. Collings, J. dePaula, G. DeCastro and E. J. Gibbs, *Biophys. J.*, 2000, **79**, 550–560.
57 M. A. Castriciano, A. Romeo and L. Monsù Scolaro, *J. Porphyrins Phthalocyanines*, 2002, **6**, 431–438.
58 R. F. Pasternack, C. Fleming, S. Herring, P. J. Collings, J. dePaula, G. DeCastro and E. J. Gibbs, *Biophys. J.*, 2000, **79**, 550–560.
59 R. F. Pasternack, S. Ewen, A. Rao, A. S. Meyer, M. A. Freedman, P. J. Collings, S. L. Frey, M. C. Ranen and J. C. dePaula, *Inorg. Chim. Acta*, 2001, **317**, 59–71.
60 (*a*) N. Micali, F. Mallamace, A. Romeo, R. Purrello and L. Monsù Scolaro, *J. Phys. Chem. B*, 2000, **104**, 5897–5904; (*b*) L. Monsù Scolaro, M. Castriciano, A. Romeo, A. Mazzaglia, F. Mallamace and N. Micali, *Physica A*, 2002, **304**, 158–169; (*c*) F. Mallamace, L. Monsù Scolaro, A. Romeo and N. Micali, *Phys. Rev. Lett.*, 1999, **82**, 3480–3483.
61 L. Monsù Scolaro, A. Romeo, M. A. Castriciano and N. Micali, *Chem. Commun.*, 2005, 3018–3020.
62 (*a*) R. F. Pasternack, S. Guerrieri, R. Lauceri and R. Purrello, *Inorg. Chim. Acta*, 1996, **246**, 7–12; (*b*) R. F. Pasternack, E. J. Gibbs, P. J. Collings, J. C. dePaula, L. C. Turzo and A. Terracina, *J. Am. Chem. Soc.*, 1998, **120**, 5873–5878; (*c*) R. F. Pasternack, S. Ewen, A. Rao, A. S. Meyer, M. A. Freedman, P. J. Collings, S. L. Frey, M. C. Ranen and J. C. dePaula, *Inorg. Chim. Acta*, 2001, **317**, 59–71; (*d*) R. F. Pasternack, E. J. Gibbs, D. Bruzewicz, D. Stewart and K. S. Engstrom, *J. Am. Chem. Soc.*, 2001, **124**, 3533–3539; (*e*) N. E. Mukundan, G. Pethö, D. W. Dixon, M. S. Kim and L. G. Marzilli, *Inorg. Chem.*, 1994, **33**, 4676–4687; (*f*) R. Purrello, L. Monsù Scolaro, E. Bellacchio, S. Guerrieri and A. Romeo, *Inorg. Chem.*, 1998, **37**, 3647–3648; (*g*) R. Purrello, E. Bellacchio, S. Guerrieri, R. Lauceri, A. Raudino, L. Monsù Scolaro and A. M. Santoro, *J. Phys. Chem. B*, 1998, **102**, 8852–8857; (*h*) E. Bellacchio, R. Lauceri, S. Guerrieri, L. Monsù Scolaro, A. Romeo and R. Purrello, *J. Am. Chem. Soc.*, 1998, **120**, 12353–12354; (*i*) R. Purrello, A. Raudino, L. Monsù Scolaro, A. Loisi, E. Bellacchio and R. Lauceri, *J. Phys. Chem. B*, 2000, **104**, 10900–10908; (*j*) R. Lauceri, A. Raudino, Monsù Scolaro, N. Micali and R. Purrello, *J. Am. Chem. Soc.*, 2002, **124**, 894–895; (*k*) T. Nezu and S. Ikeda, *Bull. Chem. Soc. Jpn.*, 1993, **66**, 25–31; (*l*) T. Nezu and S. Ikeda, *Bull. Chem. Soc. Jpn.*, 1993, **66**, 18–24.
63 (*a*) H.-y. Liu, J.-w. Huang, X. Tian, X.-d. Jiao and L.-n. Ji, *Chem. Commun.*, 1997, 1575–1576; (*b*) Y. Kubo, T. Ohno, J.-i. Yamanaka, S. Tokita, T. Iida and Y. Ishimaru, *J. Am. Chem. Soc.*, 2001, **123**, 12700–12701; (*c*) V. V. Borovkov, G. A. Hembury and Y. Inoue, *Acc. Chem. Res.*, 2004, **37**, 449–459; (*d*) V. Borovkov, T. Harada, G. A. Hembury, Y. Inoue and R. Kuroda, *Angew. Chem., Int. Ed.*, 2003, **42**, 1746–1749.
64 (*a*) R. Rubires, J.-A. Farrera and J. M. Ribó, *Chem.–Eur. J.*, 2001, **7**, 436–446; (*b*) J. M. Ribó, J. Crusats, F. Sagués, J. M. Claret and R. Rubires, *Science*, 2001, **292**, 2063–2066; (*c*) J. Crusats, J. M. Claret, I. Díez-Pérez, Z. El-Hachemi García-Ortega, R. Rubires, F. Sagués and J. M. Ribó, *Chem. Commun.*, 2003, 1588–1589.
65 J. C. de Paula, J. H. Robblee and R. F. Pasternack, *Biophys. J.*, 1995, **68**, 335–341.
66 R. F. Pasternack, J. I. Goldsmith, S. Szép and E. J. Gibbs, *Biophys. J.*, 1998, **75**, 1024–1031.
67 M. Takeuchi, S. Tanaka and S. Shinkai, *Chem. Commun.*, 2005, 5539–5541.
68 (*a*) H. Imahori, *J. Phys. Chem. B*, 2004, **108**, 6130–6143; (*b*) T. Silviu and T. S. Balaban, *Acc. Chem. Res.*, 2005, **38**, 612–623.
69 (*a*) C. F. J. Faul and M. Antonietti, *Adv. Mater.*, 2003, **15**, 673–683; (*b*) I. Goldberg, *Chem. Commun.*, 2005, 1243–1254.
70 (*a*) C. Joachim, J. K. Gimzewski and A. Aviran, *Nature*, 2000, **408**, 541–5548; (*b*) A. D. Schwab, D. E. Smith, B. Bond-Watts, D. E. Johnston, J. C. de Paula and W. F. Smith, *Nano Lett.*, 2004, **4**, 1261–1265.
71 R. Paolesse, D. Monti, L. La Monica, M. Venanzi, A. Froiio, S. Nardis, C. Di Natale, E. Martinelli and A. D'Amico, *Chem.–Eur. J.*, 2002, **8**, 2476–2483.

